Rate-Distortion and Outage Probability Analyses of Wyner-Ziv Systems over Multiple Access Channels

Shulin Song, Jiguang He, *Member, IEEE*, and Tad Matsumoto, *Life Fellow, IEEE*

***Abstract*—In this paper, we conduct rate-distortion and outage probability analyses for Wyner-Ziv (WZ) systems, where the information sequences from a source and a helper are transmitted to the destination over block Rayleigh fading multiple access channels (MACs). This work has been motivated by decision-making systems, where the aim is to make right decisions based on the observations. Hence, the most critical performance metric is the accuracy of decisions, even allowing distortion in wireless transmission. A sufficient condition for the successful transmissions is that the WZ and MAC regions intersect. For the ease of calculating the outage probability, we propose an approximated, yet accurate, WZ rate region. The outage probabilities of the WZ systems are then evaluated both in orthogonal and MAC transmissions. It is shown that the transmission efficiency of the system with MAC is significantly improved compared to orthogonal transmission. Furthermore, a helper-selection scheme is introduced to further reduce the outage probability of the WZ-MAC systems. The results show that the outage probability decreases, of which decay corresponds to the $(L+1)$-order diversity with L helpers in small value range of the average signal-to-noise ratio (SNR), while it converges into L as the average SNR becomes large.**

***Index Terms*—Wyner-Ziv problem, multiple access channel, outage probability, helper-selection, rate distortion analysis.**

I. Introduction

In the fifth generation (5G) and beyond 5G (B5G) wireless communication systems, ultra-reliable and low-latency communications (URLLC) have been considered as being of crucial importance [1], [2]. In wireless communication systems, to reasonably compromise between reliability and latency, error-control strategies such as error correction coding as well as automatic repeat request has been widely used. Nowadays, with the drastic increase in the wireless terminals and/or devices, it has been recognized that the cooperation with surrounding terminals and devices is effective to both improve the reliability and reduce the transmission latency [3], [4]. In dense terminal environments, for example, industry Internet-of-things (IoT) systems, multiple devices track the target, and send the observations to the destination, where high reliability can be achieved by the cooperation with a large number of available devices. Furthermore, if the transmissions are over multiple access channels (MACs), the latency can be significantly reduced, and thereby, the transmission efficiency improved.

On the other hand, in decision-making systems such as autonomous vehicle driving and/or unmanned factory, ultra-reliable wireless communications should not be necessarily a mandatory requirement. This is because the objective of the wireless data transfer is to provide the destination with the information required to make accurate final decisions. In this case, the destination can accept a certain level of distortion occurring in the wireless data transfer, as long as the decision results meet the reliability requirement.

Hence, we define the *global objective* of the study as analyzing the outage probability of the correlated multi-source transmissions over block fading MAC channels with distortion level as a quality-of-service (QoS) parameter. This research objective is classified into multi-source-multi-helper lossy communications with MAC transmission, which has several open questions in network information theory [12].

In [6], a lossy forward (LF) relaying system is investigated, where the relay forwards the information to the destination even though the information part may contain some errors. The original information may be recovered at the destination by joint decoding with the relay serving as a helper. To achieve lossless recovery, the rates supported by the source-destination (SD) and relay-destination (RD) links have to satisfy the Slepian-Wolf (SW) rate region with a helper, referred to as h-SW rate region. It is shown in [6] that since the information sequences transmitted over the SD and RD links are correlated, even though some errors may occur in the information part at the relay, the system coverage increases significantly compared to the conventional decode-and-forward systems. Joint decoding is utilized in LF systems to take full advantage of the correlation knowledge. However, because of the fading channel variation, the rates supported by the SD and RD links do not always fall into the admissible h-SW rate region. Zhou *et al.* [6] theoretically calculates the probability that the rate pair does not fall into the admissible h-SW rate region, which defines the outage probability of the system.

Various types of the LF systems have been investigated, which are summarized in a tutorial paper [7]. However, as described above, with the *global objective* of the decision-making systems, lossless communication should not be necessarily required. Lin *et al.* [8] analyzed the outage probability of a LF system with the end-to-end distortion level as a parameter. It is shown in [8] that if the rate pair supported by the SD and RD links satisfy the Wyner-Ziv (WZ) rate region,

Submission date for review 28/12/2020. This work was financially supported by Hitachi, Ltd..

S. Song is with Graduate School of Information Science and Technology, Hokkaido University, 5 Chome Kita 8 Jonishi, Kita-ku, Sapporo, Hokkaido, 060-0808, Japan (e-mail: shulin.song.o7@elms.hokudai.ac.jp).

J. He is with Centre for Wireless Communications, FI-90014, University of Oulu, Finland (e-mail:jiguang.he@oulu.fi).

T. Matsumoto is with IMT Atlantique Bretagne Pays de la Loire, 4 Rue Alfred Kastler, 44300 Nantes, France (e-mail: tadashi.matsumoto@imt-atlantique.fr). He is also Professor Emeritus of Japan Advanced Institute of Science and Technology (JAIST) and University of Oulu. This work was in part conducted when he was with JAIST.

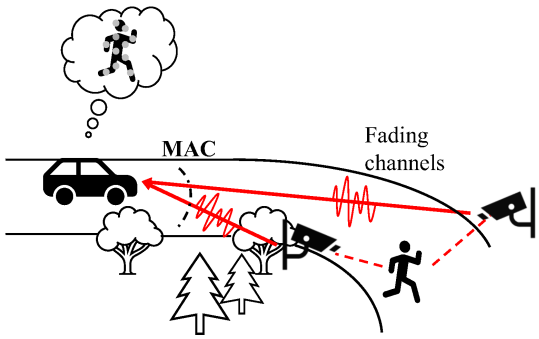

Fig. 1: Example of autonomous vehicle driving with lossy observation.

the end-to-end distortion can be made equal to or smaller than the specified level. Furthermore, the numerical results show that compared to the lossless cases, lower outage probability can be achieved. In addition, an inner bound of the rate region with one-source-multiple-helper is derived in [5]. Obviously, the more helpers, the lower the outage probability. However, the exact rate region derivation is still an open question.

Motivated by the results of [8] and the advantage of MAC over the orthogonal transmission in LF systems [7], in this paper we analyze the outage probability of one-source-one-helper lossy communication over block fading MAC channels with the end-to-end distortion level as a parameter. Even though this scenario set-up is the smallest case of the *global objective*, up to the authors' maximum knowledge, the paper for the first time provides the theoretical analysis towards achieving the *global objective*.

The results of this study can be applied to autonomous vehicle driving, as exemplified in Fig. 1, where two sensors observe the road condition, and transmit the collected data to the vehicle. The information received by the vehicle is utilized to make a decision on whether or not the vehicle should take an action to avoid the obstacles. Obviously, low latency transmission is required in this scenario to avoid the collision, for which MAC transmission is of great importance. As investigated in [9], it is shown that a sufficient condition for the lossless transmission for the correlated sources transmitted over MAC is that MAC and SW rate regions have an intersection. In [10], it is shown that the successful transmission is possible when h-SW and MAC rate regions have an intersection, which is also a sufficient condition [11]. The difference between [9] and [10] is that in [9], two sources are aimed to be reconstructed, while in [10], one of the two sources are to be reconstructed with the other serving as a helper. An obvious, but very important finding from [10] is that one-source-one-helper systems with MAC transmission can achieve twice as large transmission efficiency as its orthogonal transmission counterpart (equivalently, a half the latency) without sacrificing outage probability.

This paper aims to extend the major results of [10] to lossy cases, where the end-to-end distortion is regarded as a QoS parameter. The rates of the source and the helper should satisfy both the WZ and MAC rate regions for successful transmission with the distortion level equal to or smaller than the predefined QoS requirement, even though it is also a sufficient condition [11]. Conversely, outage probability can be evaluated as the probability that the two regions have no intersection. In this paper, the correlation between the source and the helper is expressed by the bit-flipping model, where the flipping probability is fixed as a parameter. In this case, WZ rate region is also fixed. Since the transmission links suffer from block Rayleigh fading, the MAC rate region varies, according to the variation of the instantaneous signal-to-noise ratio (SNR). Furthermore, a helper-selection scheme is introduced, where the helper-destination (HD) link with the largest instantaneous SNR is selected. The main results of this paper provide an initial solution to the *global objective*, and the major contributions are summarized as follows:

(1) For the ease of the calculations of outage probability, we propose an approximated, yet accurate, WZ rate region, with which outage probabilities in the orthogonal transmission can be derived, and a comparison is made to that derived from the exact WZ rate region.
(2) We calculate the outage probability of the WZ system in block Rayleigh fading MAC by using the approximated rate region, where the effect of helper locations is also taken into account. We also study the trade-off between the distortion and the outage probability in the MAC transmission.
(3) We also propose a helper-selection scheme in multi-helper WZ systems, of which the outage probabilities are evaluated both in orthogonal and MAC transmissions.

The rest of this paper is organized as follows: The system model of the WZ system in block Rayleigh fading MAC is introduced in Section II. We discuss the exact WZ rate region, and based on the observation of the shape of the exact WZ region, an approximated, yet accurate, WZ rate region is proposed in Section III. Furthermore, the outage probability expressions are presented in the orthogonal transmission. Section IV identifies the cases where the WZ and MAC rate regions do not intersect, resulting in the outage event in the MAC transmission. Results on the outage probability calculated by the approximated WZ rate regions in MAC are then provided, where the helper locations are taken into account. In Section V, we investigate multi-helper WZ systems with helper selection, and the outage probability is evaluated both in orthogonal and MAC transmissions. Finally, we conclude this paper in Section VI.

II. System Model

As shown in Fig. 2, two sensors observe the same target and send the observations to the destination over the MAC, where the information from one of the sensors, referred to as source, is aimed to be reconstructed, while the other serves as a helper. Let X and Y represent the information from the source and the helper, respectively, and $X^n = (X_1, X_2, \cdots, X_n)$ and $Y^n = (Y_1, Y_2, \cdots, Y_n)$ are the corresponding length-n sequences. Since the two sensors observe the same target, X and Y are correlated, of which the relationship is assumed to be described by the bit-flipping model [13], as

$$X = Y \oplus E, \tag{1}$$

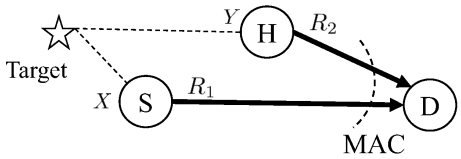

Fig. 2: One-source-one-helper Wyner-Ziv system model.

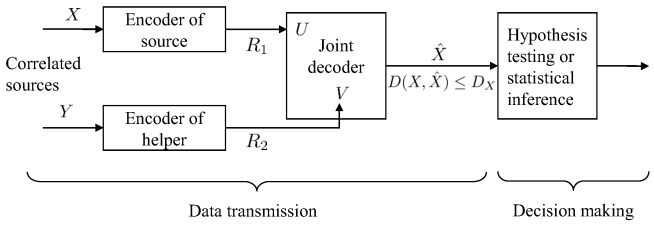

Fig. 3: Block diagram for encoder and decoder of Wyner-Ziv system followed by decision making process.

with

$$E = \begin{cases} 1, & \text{with probability } P_e, \\ 0, & \text{with probability } 1 - P_e, \end{cases} \tag{2}$$

$P_e \in [0, 0.5]$, where $P_e = 0$ and $P_e = 0.5$ represent X and Y are fully correlated and independent, respectively.

The coded and modulated sequences from the source and the helper, denoted, respectively, by $\boldsymbol{x}$ and $\boldsymbol{y}$ with the unity average signal powers, are transmitted to the destination at the rates R_1 and R_2. After joint decoding, the reconstructed information $\hat{X}$ of X can be used for decision-making, as shown in Fig. 3. Noticed that $\hat{X}$ should not necessary be exactly the same as the original information X. The distortion between X and $\hat{X}$ is defined as

$$D_X = \frac{1}{n} \sum_{j=1}^{n} d(X_j, \hat{X}_j), \tag{3}$$

where

$$d(X_j, \hat{X}_j) = \begin{cases} 1, & \text{if } X_j \neq \hat{X}_j, \\ 0, & \text{if } X_j = \hat{X}_j. \end{cases} \tag{4}$$

$D_X \in [0, 0.5]$ represents the QoS requirement of the wireless data transfer. The decisions may rely on some hypothesis testing [18] or statistical inference [19]. However, as discussed in Introduction, this paper does not intend to cover the decision making process. The requirement $D_X = 0$ refers to the lossless case and $D_X = 0.5$ refers to the case any distortion is acceptable.

The SD and HD links are assumed to suffer from block Rayleigh fading, where the channel gain stays the same within each block, and changes block-by-block. Let P_i and G_i denote the transmit power and the geometric gain [20], respectively, where the index $i \in \{1, 2\}$ refers to the SD and HD links. The received signal can be then represented as

$$\boldsymbol{z} = \sqrt{P_1 G_1} h_1 \boldsymbol{x} + \sqrt{P_2 G_2} h_2 \boldsymbol{y} + \boldsymbol{n}, \tag{5}$$

where $h_i \sim \mathcal{CN}(0, 1)$ and $\boldsymbol{n} \sim \mathcal{CN}(\mathbf{0}, \mathbf{I})$ represent the channel gain and the zero-mean complex additive white Gaussian noise (AWGN) sequences, respectively. Since shadowing is ignored for simplicity, the geometric gains can be calculated by

$$G_1 = d_{sd}^{-3.52}, \tag{6}$$

and

$$G_2 = d_{hd}^{-3.52}, \tag{7}$$

where d_{hd} and d_{sd} represent the distance of the SD and HD links, respectively. Under the assumption of normalized noise power, the average SNR is calculated by $\Gamma_i = P_i G_i$, and the instantaneous SNR is given by $\gamma_i = P_i G_i \cdot |h_i|^2$. In this paper, we assume the transmit powers of $\boldsymbol{x}$ and $\boldsymbol{y}$ are the same. Under the assumption of Rayleigh fading, the probability density function (*pdf*) of the received instantaneous SNR is given by [22]

$$p(\gamma_i) = \frac{1}{\Gamma_i} \exp\left(-\frac{\gamma_i}{\Gamma_i}\right). \tag{8}$$

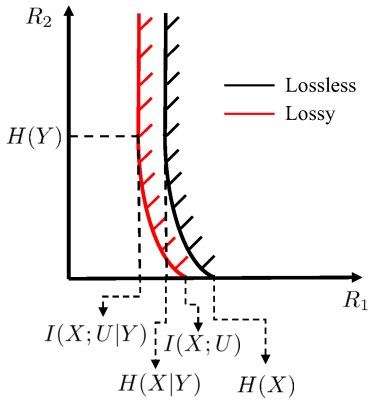

Fig. 4: Admissible rate regions of one-source-one-helper in lossless and lossy cases.

III. Wyner-Ziv Rate Region Analysis

A. Exact Wyner-Ziv Rate Regions

The rates of two distributed correlated sources, one of which serves as a helper, have to satisfy WZ rate regions in the lossy case, while h-SW rate region in the lossless case for the successful transmission [14], [15]. The admissible WZ rate region can be mathematically expressed by

$$\begin{cases} R_1 \geq I(X; U|V), \\ R_2 \geq I(Y; V), \end{cases} \tag{9}$$

where $I(\cdot;\cdot)$ indicates the mutual information between the first and second arguments. As shown in Fig. 4, the admissible rate region in the lossy case is larger than that in the lossless case. V denotes the independently decoded versions of Y, and U denotes the jointly decoded versions of X with the help of V [1]. Since $U \to X \to Y \to V$ forms a Markov chain with crossover probabilities D_X, P_e and p', $H(U|X) = H_b(D_X)$,

[1]This only describes the meaning of the inequality set in (9) and doesn't specify the decoding order in practice. As mentioned in [13], joint iterative (turbo) decoding can be used to obtain U and V. Since the channel conditions vary block-by-block, fixing decoding order is not meaningful. Since in this paper we only focus on the theoretical calculation, rather than practical implementation, the details of decoders are not investigated in this paper.

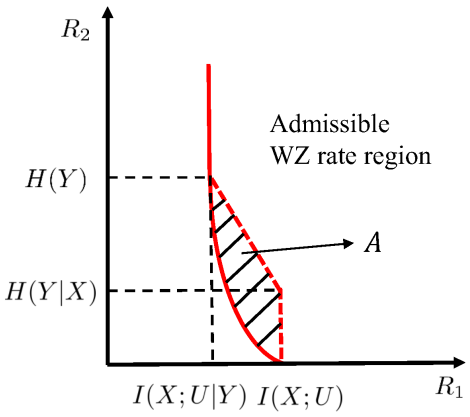

Fig. 5: Exact and approximated Wyner-Ziv rate regions; solid and doted curves represent exact and approximated rate regions, respectively.

$H(X|Y) = H_b(P_e)$ and $H(Y|V) = H_b(p')$, with $H_b(x) = -x\log_2(x) - (1-x)\log_2(1-x)$ representing the binary entropy function. Since X and Y are uniformly distributed binary sources, $H(X) = H(Y) = 1$. Hence the mutual information in (9) can be calculated by

$$\begin{aligned} I(X;U|V) &= H(U \mid V) - H(U \mid X,V) \\ &= H(U \mid V) - H(U \mid X) \\ &= H_b(D_X * P_e * p') - H_b(D_X), \end{aligned} \tag{10}$$

and

$$I(Y;V) = H(Y) - H(Y \mid V) = 1 - H_b(p'), \tag{11}$$

where the operator $*$ indicates the binary convolution $a * b = a(1-b) + b(1-a)$.

B. Approximated Wyner-Ziv Rate Regions

As discussed in Introduction, the goal of this paper is to calculate the outage probability of lossy one-source-one-helper systems in block Rayleigh fading channels. However, the exact calculation requires multi-fold integral: three-fold integral is needed in the three-node LF relay systems [15], and two-fold integral in h-SW-MAC systems [10]. Especially, as described in Section IV, the probability has to be calculated for the event that the WZ and MAC regions have an intersection when the MAC transmission is considered. Since the exact WZ rate region has a curve part, the multi-fold integral is complex. To alleviate the computational complexity, we propose an approximated, yet accurate, WZ rate region that has only lines. This idea was first proposed in [15], and its accuracy was theoretically evaluated in [6], both for the three-node lossless LF relay systems. As shown in Fig. 5, the curve part of the exact WZ rate region is approximated only by lines, with which the approximated admissible WZ rate region is expressed by

$$R_1 \geq \begin{cases} I(X;U|Y), & \text{for} \quad R_2 \geq H(Y), \\ \frac{1}{\alpha}R_2 + \frac{\beta}{\alpha}, & \text{for} \quad H(Y|X) \leq R_2 \leq H(Y), \\ I(X;U), & \text{for} \quad 0 \leq R_2 \leq H(Y|X), \end{cases} \tag{12}$$

with

$$\alpha = \frac{I(X;Y)}{I(X;U|Y) - I(X;U)}, \tag{13}$$

and

$$\beta = \frac{I(X;U) - I(X;U|Y)\cdot H(Y|X)}{I(X;U|Y) - I(X;U)}, \tag{14}$$

where

$$I(X;Y) = H(X) - H(X \mid Y) = 1 - H_b(P_e), \tag{15}$$

$$\begin{aligned} I(X;U|Y) &= H(U \mid Y) - H(U \mid X,Y) \\ &= H(U \mid Y) - H(U \mid X) \\ &= H_b(D_X * P_e) - H_b(D_X), \end{aligned} \tag{16}$$

$$I(X;U) = H(X) - H(X \mid U) = 1 - H_b(D_X), \tag{17}$$

and

$$H(Y \mid X) = H_b(P_e). \tag{18}$$

C. Outage Probability in Two-Phase Orthogonal Transmission Case

Outage is defined as the event where the rate pair does not fall into the admissible rate regions. Hence, the outage probability of one-source-one-helper WZ systems can be expressed by twofold integrals with respect to the *pdf* of the instantaneous SNRs of each link. In the case of the orthogonal transmission, the intersection of the WZ and MAC regions does not have to be taken into account. Hence, the outage probability can also be derived from the exact rate region expressed in (9). In this subsection, we first calculate the outage probability based on both (9) and the approximation (12), and then the next subsection compares the results derived from (9) and (12).

Since the SD and HD links are both point-to-point, the rate-distortion pair (R_i, D_i), $i = 1, 2$, is achievable, if Shannon's source-channel separation theorem

$$R_i(D_i)R_{c,i} \leq C(\gamma_i) \tag{19}$$

is satisfied, where $C(\gamma_i) = \log_2(1+\gamma_i)$ is the channel capacity of each link. $R_{c,i}$ denotes the normalized spectrum efficiency, of which the modulation multiplicity and the channel coding rate are taken into account [16]. $R_i(D_i)$ is the rate distortion function for lossy source coding. With the uniformly distributed binary source assumption, $R_i = 1 - H_b(D_i)$. For the information transmitted by the helper, $R_2 = 1 - H_b(p')$. Hence $p' = H_b^{-1}\{1 - R_2\} = H_b^{-1}\left\{1 - \frac{C(\gamma_2)}{R_{c,2}}\right\}$. Since the inverse of the binary entropy function $H_b^{-1}\{\cdot\}$ can not be expressed explicitly, we use the expression obtained by a curve fitting technique shown in [6], as

$$H_b^{-1}(x) \approx \left(2^{ax^b} - 2^{-cx^d}\right)^e, \tag{20}$$

where $a = 0.6794$, $b = 0.7244$, $c = 0.1357$, $d = 21.8026$ and $e = 1.9920$.

The outage probability derived from the exact WZ region in the orthogonal transmission can be expressed by $P_{out,exact} = P_{out,exact,1} + P_{out,exact,2}$, with

$$\begin{aligned}
&P_{out,exact,1}\\
&=\Pr\left\{0 \le R_1 \le I\left(X;U|Y\right); R_2 \ge 0\right\}\\
&=\Pr\left\{\Phi\left(0\right) \le \gamma_1 \le \Phi\left[I\left(X;U|Y\right)\right]; \gamma_2 \ge \Phi\left(0\right)\right\}\\
&=\int_{\Phi(0)}^{\Phi[I(X;U|Y)]}\int_{\Phi(0)}^{+\infty} p\left(\gamma_1\right)p\left(\gamma_2\right)d\gamma_2 d\gamma_1\\
&=\int_{0}^{2^{R_{c,1}\left[H_b\left(D_X*P_e\right)-H_b\left(D_X\right)\right]}-1}\int_{0}^{+\infty} p\left(\gamma_1\right)p\left(\gamma_2\right)d\gamma_2 d\gamma_1,
\end{aligned} \tag{21}$$

and

$$\begin{aligned}
&P_{out,exact,2}\\
&=\Pr\left\{I\left(X;U|Y\right) \le R_1 \le I\left(X;U|V\right); 0 \le R_2 \le H(Y)\right\}\\
&=\Pr\left\{\begin{array}{c}\Phi\left[I\left(X;U|Y\right)\right] \le \gamma_1 \ge \Phi\left[I\left(X;U|V\right)\right];\\ \Phi\left(0\right) \le \gamma_2 \le \Phi\left[H(Y)\right]\end{array}\right\}\\
&=\int_{\Phi(0)}^{\Phi[H(Y)]}\int_{\Phi[I(X;U|V)]}^{\Phi[I(X;U|V)]} p\left(\gamma_1\right)p\left(\gamma_2\right)d\gamma_1 d\gamma_2\\
&=\int_{0}^{2^{R_{c,1}}-1}\int_{2^{R_{c,2}\left[H_b\left(D_X*P_e*p'\right)-H_b\left(D_X\right)\right]}-1}^{2^{R_{c,2}\left[H_b\left(D_X*P_e\right)-H_b\left(D_X\right)\right]}-1}\\
&\quad p\left(\gamma_1\right)p\left(\gamma_2\right)d\gamma_1 d\gamma_2,
\end{aligned} \tag{22}$$

where the relationship between the rate and the instantaneous SNR is given by

$$\gamma_i = \Phi\left(R_i\right) = 2^{R_{c,i}R_i} - 1, \tag{23}$$

and

$$R_i = \Phi^{-1}\left(\gamma_i\right) = \frac{1}{R_{c,i}}\log_2\left(1+\gamma_i\right). \tag{24}$$

The outage probability with the approximated WZ region in orthogonal transmission is expressed by $P_{out,approx} = P_{out,approx,1} + P_{out,approx,2}$, with

$$\begin{aligned}
&P_{out,approx,1}\\
&=\Pr\left\{0 \le R_1 \le I\left(X;U|Y\right); R_2 \ge 0\right\}\\
&=\Pr\left\{\Phi\left(0\right) \le \gamma_1 \le \Phi\left[I\left(X;U|Y\right)\right]; \gamma_2 \ge \Phi\left(0\right)\right\}\\
&=\int_{\Phi(0)}^{\Phi[I(X;U|Y)]}\int_{\Phi(0)}^{+\infty} p\left(\gamma_1\right)p\left(\gamma_2\right)d\gamma_2 d\gamma_1\\
&=\int_{0}^{2^{R_{c,1}\left[H_b\left(D_X*P_e\right)-H_b\left(D_X\right)\right]}-1}\int_{0}^{+\infty} p\left(\gamma_1\right)p\left(\gamma_2\right)d\gamma_2 d\gamma_1,
\end{aligned} \tag{25}$$

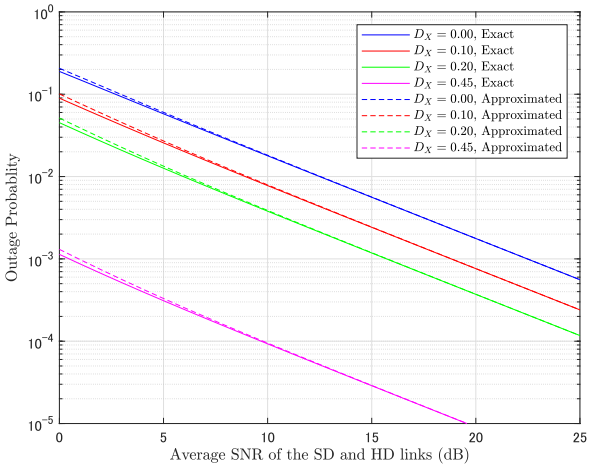

Fig. 6: Outage probabilities calculated from exact and approximated WZ rate regions in two-phase orthogonal transmission.

and

$$\begin{aligned}
&P_{out,approx,2}\\
&=\Pr\left\{I\left(X;U|Y\right) \le R_1 \le I\left(X;U\right); 0 \le R_2 \le \alpha R_1 - \beta\right\}\\
&=\Pr\left\{\begin{array}{c}\Phi\left[I\left(X;U|Y\right)\right] \le \gamma_1 \le \Phi\left[I\left(X;U\right)\right];\\ \Phi\left(0\right) \le \gamma_2 \le \Phi\left(\alpha R_1 - \beta\right)\end{array}\right\}\\
&=\int_{\Phi[I(X;U|Y)]}^{\Phi[I(X;U)]}\int_{\Phi(0)}^{\Phi(\alpha R_1-\beta)} p\left(\gamma_1\right)p\left(\gamma_2\right)d\gamma_2 d\gamma_1\\
&=\int_{2^{R_{c,1}\left[H_b\left(D_X*P_e\right)-H_b\left(D_X\right)\right]}-1}^{2^{R_{c,1}\left[1-H_b\left(D_X\right)\right]}-1}\int_{0}^{2^{-R_{c,2}\beta}\left(1+\gamma_1\right)^{\frac{R_{c,2}}{R_{c,1}}\alpha}-1}\\
&\quad p\left(\gamma_1\right)p\left(\gamma_2\right)d\gamma_2 d\gamma_1.
\end{aligned} \tag{26}$$

D. Comparison of Outage Probabilities in Orthogonal Transmission

According to the expressions provided in Subsection III-C, this subsection compares the outage probabilities derived from the exact and approximated WZ rate regions in the orthogonal transmission. Without loss of generality, $R_{c,1} = R_{c,2} = 0.5$ is assumed throughout this paper. As shown in Fig. 6, the solid curves represent the outage probability obtained by the exact WZ rate region, while the dotted curves denote that obtained by the approximated WZ rate region. The results indicate that the difference is negligibly small. It is found that the smaller the gap, the larger the average SNR as well as the smaller the D_X. It is also found that even though the gap is small, the outage probability derived from the approximated WZ region is slightly larger than that derived from the exact region. This is because the probability that the rate pair falls into the area indicated by A in Fig. 5 is ignored in the approximation. It can be concluded that the approximation is very accurate. Hence, we utilize the approximated WZ rate region in WZ-MAC outage probability analysis.

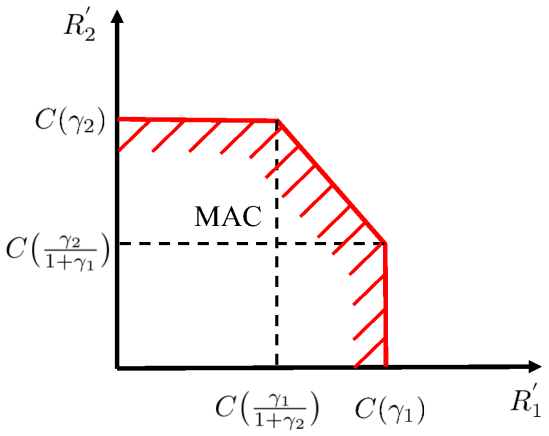

Fig. 7: MAC rate region.

IV. Outage Probability Analysis in One-phase MAC

A. MAC Rate Region

Since the information from the source and the helper is assumed to be transmitted over the MAC, the transmission rates have to satisfy MAC rate region for successful transmissions, as shown in Fig. 7. The achievable MAC rate region can be expressed by

$$\begin{cases} {R_1}' \le C(\gamma_1), \\ {R_2}' \le C(\gamma_2), \\ {R_1}' + {R_2}' \le C(\gamma_1+\gamma_2). \end{cases} \tag{27}$$

In the WZ systems, MAC transmission is successful when the WZ and MAC rate regions intersect, with which source-channel separation holds, since the rate pair is included in the both regions. Replacing ${R_i}'$ in (27) with $R_i R_{c,i}$, the MAC region with the source-channel separation can be further represented by

$$\begin{cases} R_1 R_{c,1} \le C(\gamma_1), \\ R_2 R_{c,2} \le C(\gamma_2), \\ R_1 R_{c,1} + R_2 R_{c,2} \le C(\gamma_1+\gamma_2). \end{cases} \tag{28}$$

B. Outage Probability Expressions in MAC Case

The outage probability can be calculated by twofold integrals, of which the boundaries are determined by the admissible rate regions. For the ease of twofold integral calculations, we use the approximated WZ rate region. Two scenarios with which outage happens are shown in Fig. 8. The outage probability can be expressed by $P_{out,MAC} = P_{out,MAC,1} + P_{out,MAC,2}$. In Fig. 8a, since $\frac{1}{R_{c,1}} C(\gamma_1) \le I(X;U|Y)$, the

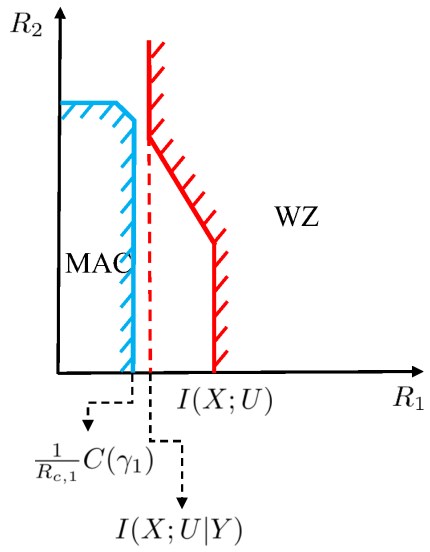

(a) Scenario for $P_{out,MAC,1}$

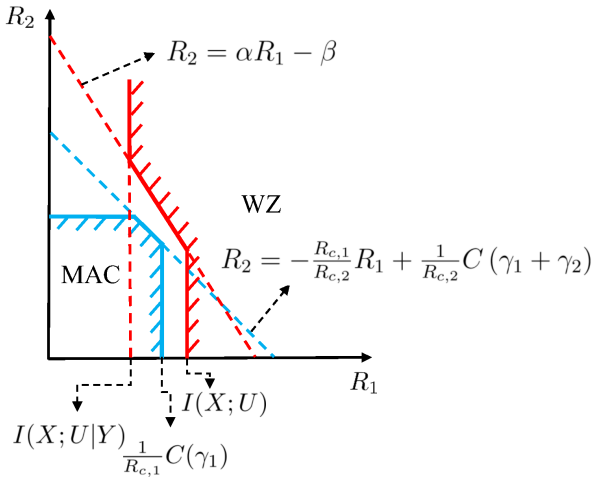

(b) Scenario for $P_{out,MAC,2}$

Fig. 8: Two scenarios that WZ and MAC rate regions do not intersect.

WZ and MAC regions do not intersect. Hence,

$$\begin{aligned} &P_{out,MAC,1} \\ &= \Pr\left\{0 \le \frac{1}{R_{c,1}} C(\gamma_1) \le I(X;U|Y); \frac{1}{R_{c,2}} C(\gamma_2) \ge 0\right\} \\ &= \Pr\{\Phi(0) \le \gamma_1 \le \Phi[I(X;U|Y)]; \gamma_2 \ge \Phi(0)\} \\ &= \int_{\Phi(0)}^{\Phi[I(X;U|Y)]} \int_{\Phi(0)}^{+\infty} p(\gamma_1) p(\gamma_2) d\gamma_2 d\gamma_1 \\ &= \int_0^{2^{R_{c,1}[H_b(D_X * P_e) - H_b(D_X)]} - 1} \int_0^{+\infty} p(\gamma_1) p(\gamma_2) d\gamma_2 d\gamma_1. \end{aligned} \tag{29}$$

In Fig. 8b, with $I(X;U|Y) \le \frac{1}{R_{c,1}} C(\gamma_1) \le I(X;U)$, the regions do not intersect when $0 \le -\frac{R_{c,1}}{R_{c,2}} R_1 +$

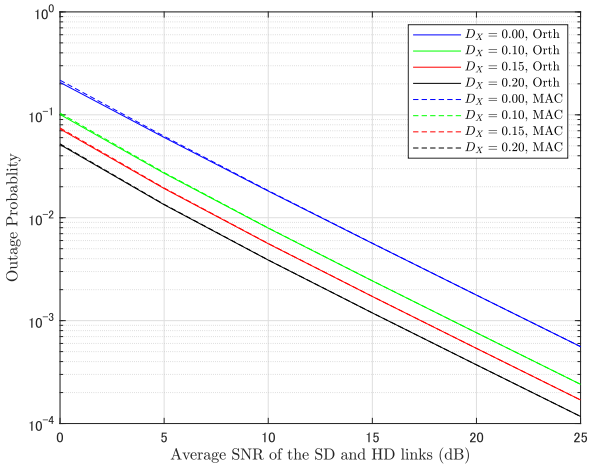

Fig. 9: Outage probabilities of WZ systems in two-phase orthogonal and one-phase MAC transmissions for $P_e = 0.1$.

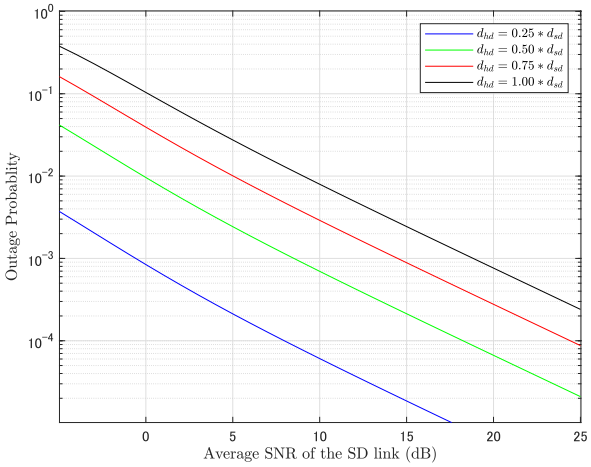

Fig. 10: Outage probability with different helper locations $d_{hd} = \theta \cdot d_{sd}$, $\theta \in \{0.25, 0.5, 0.75, 1.0\}$.

$\frac{1}{R_{c,2}} C(\gamma_1 + \gamma_2) \leq \alpha R_1 - \beta$. Hence,

$$
\begin{aligned}
& P_{out,MAC,2} \\
&= \Pr\left\{ \begin{array}{c} I(X;U|Y) \leq \frac{1}{R_{c,1}} C(\gamma_1) \leq I(X;U); \\ 0 \leq -\frac{R_{c,1}}{R_{c,2}} R_1 + \frac{1}{R_{c,2}} C(\gamma_1 + \gamma_2) \leq \alpha R_1 - \beta \end{array} \right\} \\
&= \Pr\left\{ \begin{array}{c} \Phi[I(X;U|Y)] \leq \gamma_1 \leq \Phi[I(X;U)]; \\ \Phi(0) \leq \gamma_2 \leq M \end{array} \right\} \\
&= \int_{\Phi[I(X;U|Y)]}^{\Phi[I(X;U)]} \int_{\Phi(0)}^{M} p(\gamma_1) p(\gamma_2) d\gamma_2 d\gamma_1 \\
&= \int_{2^{R_{c,1}[H_b(D_X * P_e) - H_b(D_X)]} - 1}^{2^{R_{c,1}[1 - H_b(D_X)]} - 1} \int_{0}^{M} p(\gamma_1) p(\gamma_2) d\gamma_2 d\gamma_1,
\end{aligned}
\tag{30}
$$

with $M = 2^{-\beta R_{c,2}} (1 + \gamma_1)^{\left(\frac{\alpha R_{c,2}}{R_{c,1}} + 1\right)} - 1 - \gamma_1$.

C. Numerical Results of Outage Probability in One-Phase MAC Transmission

According to the expressions provided in Subsection IV-B, numerical results of the outage probabilities are presented in this subsection. We first compare the outage probabilities of two sources transmitted using one transmission phase with MAC and using two orthogonal transmission phases. This comparison is fair because their transmit powers are the same. Fig. 9 shows the outage probabilities of WZ systems in the orthogonal and MAC transmissions, with the distortion D_X as a parameter. The results show that the difference is negligibly small. However, the transmission efficiency in the MAC transmission is twice as large as that in the orthogonal transmission, i.e., two phases are needed to transmit the source and helper information independently by using orthogonal transmission, while only one phase by MAC.

We also take into account the effect of the helper locations on the outage probability, where $d_{hd} = \theta \cdot d_{sd}$ with $\theta \in (0, 1]$. Since d_{sd} is normalized to the unity, the geometric gain makes change to the average SNR of the HD link, and is expressed as $G_2 = \theta^{-3.52}$ [21]. Fig. 10 shows the outage probability with θ as a parameter. Obviously, it is found that the outage probability decreases with smaller θ since the distance between the helper and the destination decreases.

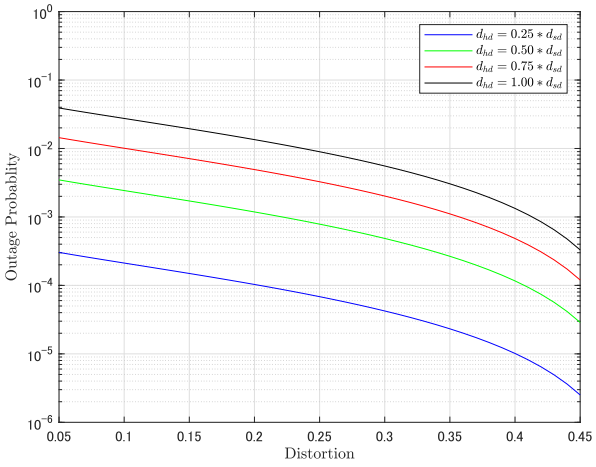

Fig. 11: Relationship between outage probability and distortion for $\theta \in \{0.25, 0.5, 0.75, 1.0\}$ with the average SNR of the SD link is 5 dB.

We also investigate the relationship between the outage probability and the distortion. It is found in Fig. 11 that the larger the acceptable distortion, the smaller the outage probability. When the acceptable distortion is larger than 0.35, the outage probability decrease more rapidly, of which the tendency is consistent to [8]. Also, lower outage probability can be achieved when the distance between the helper and the destination decreases. Fig. 11 suggests that the trade-off between the distortion and the outage probability can be well controlled, and the required average SNR to satisfy the outage probability requirement can be identified.

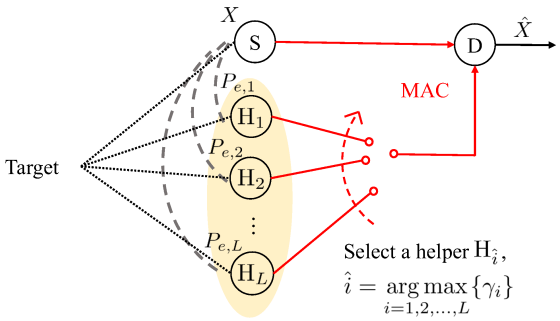

Fig. 12: Helper-selection WZ system.

V. WZ Systems with Helper Selection

A. WZ Systems with Helper Selection

We investigate a one-source-multi-helper system in this section, where a helper-selection technique is introduced. As shown in Fig. 12, since one source and L helpers observe the same target, the information obtained by the source and helpers is correlated. Instead of sending information from all the helpers H_i, $i = 1, 2, ..., L$, the best helper $H_{\hat{i}}$ is assumed to be selected with the help of higher layer protocols which is, however, not detailed at this stage of the paper. Let $P_{e,i}$ represents the crossover probability of the information between the source and the helper H_i, and p_i denote the crossover probability between the original and decoded information via the i-th HD link. The best helper $H_{\hat{i}}$ has to satisfy [24]

$$\hat{i} = \arg\min_i \{P_{e,i} * p_i\}, \tag{31}$$

where $P_{e,i}$ is set as a fixed parameter while p_i is a random variable depending on the instantaneous SNR of the HD link. Even though finding the best helper following (31) may be possible with the help of higher layer protocol, it is not practical in the systems requiring low latency.

Even though in practice $P_{e,i}$ is a random variable, because of the justification provided in Appendix A, we assume $P_{e,i} = P_{e,max}$, $i = 1, 2, ..., L$ [2], even though they are random variable. With this assumption, the best helper $H_{\hat{i}}$ to be selected should be the one having the largest instantaneous SNR, as [3]

$$\hat{i} = \arg\max_i \{\gamma_i\}. \tag{32}$$

The source and the selected helper then transmit their observations over MAC. One-source-multiple-helper with helper selection can be seen as a simple solution to one-source-multi-helper problems. The *pdf* of the instantaneous SNR in Rayleigh fading with helper selection is equivalent to the selection combining diversity, expressed as [25]

$$p_s(\gamma_2) = \frac{L}{\Gamma_2} \exp\left(-\frac{\gamma_2}{\Gamma_2}\right) \left[1 - \exp\left(-\frac{\gamma_2}{\Gamma_2}\right)\right]^{L-1}. \tag{33}$$

[2]This assumption is reasonable because the $P_{e,i}$ value determines the average SNR value where the diversity order changes from $L+1$ to L. Obviously, the decrease in the diversity order changes the decay of the curve of outage probability versus the average SNR. However, since the more the helpers, the sharper the decay, the average SNR corresponding to the decay change can not be clearly identified. Under this assumption, the outage probabilities shown in Fig. 13 and Fig. 14 are upper bounds, according to Appendix A which investigates the effect of the correlation between the source and the helpers in helper-selection WZ systems in two extreme cases.

[3]For example, a short packet is transmitted to the destination sequentially from all the helpers during the 'monitoring phase' in the protocol. The destination identifies which helper's received instantaneous SNR is the largest, and requests the best helper for the transmission. This 'monitoring phase' does not reduce the overall throughput significantly.

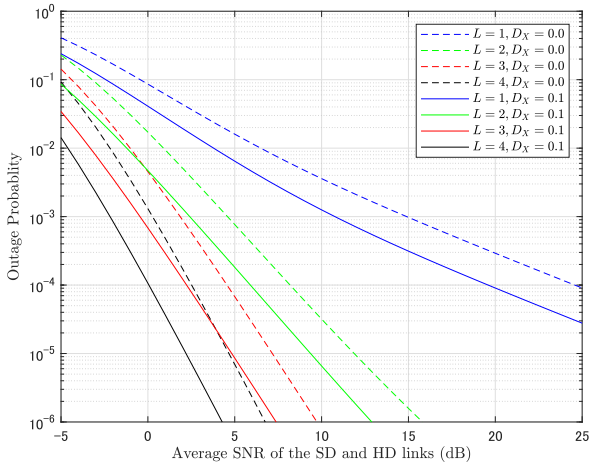

Fig. 13: Outage probabilities of WZ with helper selection in both lossless and lossy two-phase orthogonal transmissions for $P_{e,i} = 0.01$.

B. Outage Probability Calculation Results

The outage probability of the helper-selection WZ systems in the orthogonal and MAC transmissions can be obtained by repacing the *pdf* $p(\gamma_2)$ by $p_s(\gamma_2)$ in (25), (26), (29) and (30). In Fig. 13, outage probabilities of the helper-selection WZ systems with the orthogonal transmission in both lossless and lossy cases are presented. The result indicates that with the lossy transmission, lower outage probability can be achieved. It is found that the outage probability decreases, of which decay corresponds to the $(L+1)$-order diversity with L helpers in a small value range of the average SNR, while it converges into L as the average SNR becomes large. This is because the source and helper information is not fully correlated ($P_{e,i} \neq 0$).

According to the numerical results, we make a comparison of the outage probability of the helper-selection WZ systems in the orthogonal and MAC transmissions. As shown in Fig. 14, the difference in outage probability between the orthogonal and MAC transmissions is negligibly small. Hence, the transmission efficiency with MAC can be improved without sacrificing outage probability. In both cases, the diversity order with helper selection is $L+1$ when the average SNR is small and approaches L when the average SNR becomes large. It should be noted that Fig. 14 does not take account the overhead due to the help of the higher layer protocol.

VI. Conclusion

In this paper, the outage probabilities of WZ systems both in the orthogonal and MAC transmissions have been evaluated.

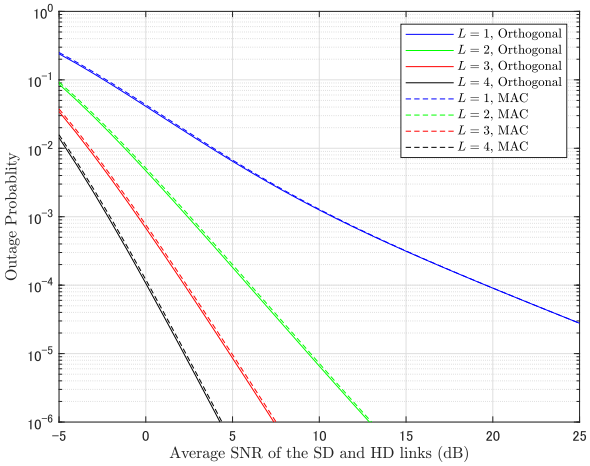

Fig. 14: Outage probability of helper-selection WZ systems in two-phase orthogonal and one-phase MAC transmissions for $P_{e,i} = 0.01$ and $D_X = 0.1$.

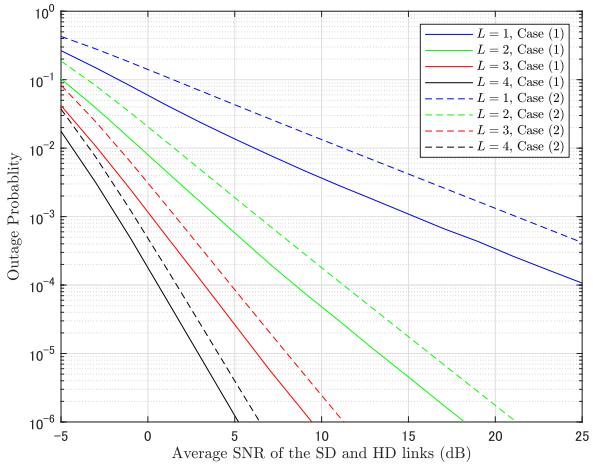

Fig. 15: Outage probability of helper-selection one-phase MAC WZ system in two extreme cases for $P_{e,max} = 0.2$ and $D_X = 0.1$.

For MAC transmission, we defined successful transmissions as the case the WZ and MAC rate regions intersect. Conversely, outage happens when they have no intersection. In order to make the outage probability calculations tractable, an approximation of WZ rate region has been proposed. The results have demonstrated that the difference in outage probabilities between the exact and approximated WZ regions is negligibly small. It has been found that compared to lossless transmissions, lower outage probability can be achieved in lossy transmissions, and the larger the acceptable distortion, the lower the outage probability. In addition, when the helper is located closer to the destination, outage probability decreases. Furthermore, we have investigated the WZ systems with helper selection, of which the outage probabilities both in the orthogonal and MAC transmissions are theoretically calculated. The results show that the outage probability decreases, of which decay corresponds to the $(L+1)$-order diversity with L helpers in a small value range of the average SNR, while it converges into L as the average SNR becomes large. It has been verified that without sacrificing outage probability, the transmission efficiency in the MAC transmission is twice as large as that in the orthogonal transmission in one-source-one-helper and helper-selection WZ systems.

APPENDIX

In practice, since the relative positions of the source and the helpers are not the same, $P_{e,i}$ is a random variable. It *may* be reasonable to assume $P_{e,i}$ follows the uniform distribution, where the maximum value is $P_{e,max}$. To evaluate the effect of the correlation between the source and the helper, two extreme cases are considered:

Case (1): the first helper has the lowest correlation to the source, and the other helper are fully correlated to the source, as

$$P_{e,i} = \begin{cases} P_{e,max}, & \text{for} \quad i = 1, \\ 0, & \text{for} \quad i = 2, 3, ..., L. \end{cases} \tag{34}$$

Case (2): all of the helpers have the lowest correlation, as

$$P_{e,i} = P_{e,max}, \text{ for } i = 1, 2, ..., L, \tag{35}$$

which is the assumption used in Section V.

Numerical results of the outage probabilities for Case (1) and (2) with $P_{e,max} = 0.2$ and $D_X = 0.1$ are shown in Fig. 15. It is found that the outage probability curves with the assumption of (35) are above that with (34) for all the considered L values. Hence, the assumption of (35) yields the upper bound of the outage probability. It is important to see that the gap between the two cases becomes smaller with larger L. This observation inherently justifies the statements described in *footnote 1*, and hence, the assumption of $P_{e,i} = P_{e,max}$, $i = 1, 2, ..., L$ in the outage probability analysis is indirectly proven to be reasonable.

REFERENCES

[1] C. Li, J. Jiang, W. Chen, T. Ji and J. Smee, "5G ultra-reliable and low-latency systems design," in *European Conference on Networks and Communications (EuCNC)*, Oulu, 2017, pp. 1-5.

[2] I. Parvez, A. Rahmati, I. Guvenc, A. I. Sarwat and H. Dai, "A survey on low latency towards 5G: RAN, core network and caching solutions," *IEEE Commun. Surv. Tutor.*, vol. 20, no. 4, pp. 3098-3130, Fourthquarter 2018.

[3] P. Popovski et al., "Wireless access for ultra-reliable low-latency communication: principles and building blocks," *IEEE Network*, vol. 32, no. 2, pp. 16-23, March-April 2018.

[4] J. He, V. Tervo, S. Qian, Q. Xue, M. Juntti and T. Matsumoto, "Performance analysis of lossy decode-and-forward for non-orthogonal MARCs," *IEEE Trans. Commun.*, vol. 17, no. 3, pp. 1545-1558, March 2018.

[5] W. Lin and T. Matsumoto, "Performance analysis of distortion-acceptable cooperative communications in wireless sensor networks for internet of things," *IEEE Sens. J.*, vol. 19, no. 5, pp. 1979-1989, 1 March1, 2019.

[6] X. Zhou, M. Cheng, X. He and T. Matsumoto, "Exact and approximated outage probability analyses for decode-and-forward relaying system allowing intra-link errors," *IEEE Trans. Commun.*, vol. 13, no. 12, pp. 7062-7071, Dec. 2014.

[7] J. He et al., "A tutorial on lossy forwarding cooperative relaying," *IEEE Commun. Surv. Tutor.*, vol. 21, no. 1, pp. 66-87, Firstquarter 2019.

[8] W. Lin, S. Qian and T. Matsumoto, "Lossy-forward relaying for lossy communications: rate-distortion and outage probability analyses," *IEEE Trans. Commun.*, vol. 18, no. 8, pp. 3974-3986, Aug. 2019.

[9] X. Zhou, X. He, M. Juntti and T. Matsumoto, "Outage probability of correlated binary source transmission over fading multiple access channels," in *IEEE 16th International Workshop on Signal Processing Advances in Wireless Communications (SPAWC)*, Stockholm, pp. 96-100, 2015.
[10] S. Song, M. Cheng, J. He, X. Zhou and T. Matsumoto, "Outage probability of one-source-with-one-helper sensor systems in block Rayleigh fading multiple access channels," *IEEE Sens. J.*, vol. 21, no. 2, pp. 2140-2148, 15 Jan.15, 2021.
[11] R. Rajesh and V. Sharma, "Transmission of correlated sources over a fading multiple access channel," in *Communication, Control, and Computing, 2008 46th Annual Allerton Conference*, pp. 858–864, 2008.
[12] A. E. Gamal and Y. H. Kim, "Network information theory," *Cambridge Univ. Press*, 2011.
[13] K. Anwar and T. Matsumoto, "Accumulator-assisted distributed turbo codes for relay systems exploiting source-relay correlation," *IEEE Commun. Lett.*, vol. 16, no. 7, pp. 1114–1117, Jul. 2012.
[14] D. Slepian and J. Wolf, "Noiseless coding of correlated information sources," *IEEE Trans. Inf. Theory*, vol. 19, no. 4, pp. 471-480, July 1973.
[15] M. Cheng, K. Anwar, and T. Matsumoto, "Outage probability of a relay strategy allowing intra-link errors utilizing Slepian-Wolf theorem," *EURASIP J. Adv. Signal Process.*, vol. 2013, no. 1, pp. 22-34, 2013.
[16] J. G. Frias and Y. Zhao, "Near-Shannon/Slepian-Wolf performance for unknown correlated sources over AWGN channels," *IEEE Trans. Commun.*, vol. 53, no. 4, pp. 555–559, Apr. 2005.
[17] D. Slepian and J. Wolf, "Noiseless coding of correlated information sources," *IEEE Trans. Inf. Theory*, vol. IT-19, no. 4, pp. 471-480, Jul. 1973.
[18] H. Shimokawa, T. S. Han and S. Amari, "Error bound of hypothesis testing with data compression," in 1994 *IEEE International Symposium on Information Theory*, Trondheim, Norway, 1994, pp. 114.
[19] D. J. C. Mackay, "Information theory, inference, and learning algorithms" *Cambridge Univ. Press*, 2003.
[20] H. Ochiai, P. Mitran and V. Tarokh, "Design and analysis of collaborative diversity protocols for wireless sensor networks," in *IEEE 60th Vehicular Technology Conference*, Los Angeles, CA, 2004, pp. 4645-4649.
[21] R. Youssef and A. G. I. Amat, "Distributed serially concatenated codes for multi-source cooperative relay networks," *IEEE Trans. Commun.*, vol. 10, no. 1, pp. 253-263, January 2011.
[22] M. Schwartz, W. R. Bennett, and S. Stein, "Communication systems and techniques," *IEEE Commun. Mag.*, vol. 34, no. 5, pp. 9-10, May 1996.
[23] C. E. Shannon, "Coding theorems for a discrete source with a fidelity criterion," *IRE Nat. Conv. Rec*, vol. 4, no. 1, pp. 142-163, 1959.
[24] J. Hu and N. C. Beaulieu, "Performance analysis of decode-and-forward relaying with selection combining," *IEEE Commun. Lett.*, vol. 11, no. 6, pp. 489-491, June 2007.
[25] A. Goldsmith, "Wireless communications" *Cambridge Univ. Press*, 2005.

Shulin Song received the B.S. degree from Xi'an University of Posts and Telecommunications, Xi'an, China, in 2018, and the M.S. degree from Japan Advanced Institute of Science and Technology (JAIST), Ishikawa, Japan, in 2020. She is currently pursuing a Ph.D. degree in Hokkaido University, Sapporo, Japan. Her research interests include Information Theory, Network Information Theory, Communication Theory, Cooperative Communications and Non-orthogonal Multiple Access.

Jiguang He received the B.Eng. degree from the Harbin Institute of Technology, Harbin, China, in 2010, the M.Sc. degree from Xiamen University, Xiamen, China, in 2013, and the D.Sc. degree from the University of Oulu, Oulu, Finland, in 2018, all in communications engineering. From September 2013 to March 2015, he was with the Key Laboratory of Millimeter Waves, City University of Hong Kong, and conducting research on channel tracking over millimeter wave MIMO systems. Since June 2015, he has been with the Centre for Wireless Communications (CWC), University of Oulu. His research interests span cooperative communications, network information theory, joint source and channel coding, and distributed compressive sensing.

Tad Matsumoto (S'84-M'98-F'10) received his B.S. and M.S. degrees in electrical engineering, and his Ph.D. degree in electrical engineering, all from Keio University, Yokohama, Japan, in 1978, 1980, and 1991, respectively. He joined Nippon Telegraph and Telephone Corporation (NTT), in 1980, where he was involved in a lot of research and development projects mobile wireless communications systems. In 1992, he transferred to NTT DoCoMo, where he researched on code-division multiple-access techniques for mobile communication systems. In 1994, he transferred to NTT America, where he served as a Senior Technical Advisor of a joint project between NTT and NEXTEL Communications. In 1996, he returned to NTT DoCoMo, where he served as the Head of the Radio Signal Processing Laboratory, until 2001. He researched on adaptive signal processing, multiple-input multiple-output turbo signal detection, interference cancellation, and space-time coding techniques for broadband mobile communications. In 2002, he moved to the University of Oulu, Finland, where he served as a Professor at Centre for Wireless Communications. In 2006, he has served as a Visiting Professor with the Ilmenau University of Technology, Ilmenau, Germany, supported by the German MERCATOR Visiting Professorship Program. Since 2007, he has been serving as a Professor with the Japan Advanced Institute of Science and Technology (JAIST), Japan, while also keeping a cross-appointment position with the University of Oulu. After his retirement from JAIST, he moved to IMT-Atlantic, France, where he is serving as an invited professor. He is also Professor Emeritus of JAIST and University of Oulu. Prof. Matsumoto is a member of the IEICE. He has led a lot of projects supported by the Academy of Finland, European FP7, and the Japan Society for the Promotion of Science and Japanese private companies. He has been appointed as a Finland Distinguished Professor, from 2008 to 2012, supported by Finnish National Technology Agency (Tekes) and Finnish Academy, under which he preserves the rights to participate in and apply for European and Finnish National Projects. He was a recipient of IEEE VTS Outstanding Service Award, in 2001, Nokia Foundation Visiting Fellow Scholarship Award, in 2002, IEEE Japan Council Award for Distinguished Service to the Society, in 2006, the IEEE Vehicular Technology Society James R. Evans Avant Garde Award, in 2006, Thuringen State Research Award for Advanced Applied Science, in 2006, the 2007 Best Paper Award of the Institute of Electrical, Communication, and Information Engineers of Japan, in 2008, Telecom System Technology Award from the Telecommunications Advancement Foundation, in 2009, IEEE Communication Letters Exemplary Reviewer, in 2011, Nikkei Wireless Japan Award, in 2013, IEEE VTS Recognition for Outstanding Distinguished Lecturer, in 2016, and IEEE TRANSACTIONSON COMMUNICATIONS Exemplary Reviewer, in 2018. He has been serving as an IEEE Vehicular Technology Distinguished Speaker, since 2016.